

See discussions, stats, and author profiles for this publication at: <https://www.researchgate.net/publication/259335720>

Structural Dynamics in a "Breathing" Metal –Organic Framework Studied by Electron Paramagnetic Resonance of Nitroxide Spin Probes

DATASET *in* JOURNAL OF PHYSICAL CHEMISTRY LETTERS · DECEMBER 2013

Impact Factor: 7.46 · DOI: 10.1021/jz402357v

CITATIONS

7

READS

116

10 AUTHORS, INCLUDING:



Daniil Kolokolov

Boreskov Institute of Catalysis

28 PUBLICATIONS 305 CITATIONS

SEE PROFILE



Anton Gabrienko

Boreskov Institute of Catalysis

27 PUBLICATIONS 238 CITATIONS

SEE PROFILE



Alexander G Stepanov

Boreskov Institute of Catalysis

136 PUBLICATIONS 1,681 CITATIONS

SEE PROFILE



E.G. Bagryanskaya

Novosibirsk Institute of Organic Chemistry

136 PUBLICATIONS 1,542 CITATIONS

SEE PROFILE

Structural Dynamics in a “Breathing” Metal–Organic Framework Studied by Electron Paramagnetic Resonance of Nitroxide Spin Probes

Alena M. Sheveleva,^{†,‡} Daniil I. Kolokolov,^{||,‡} Anton A. Gabrienko,^{||} Alexander G. Stepanov,^{||,‡} Sergey A. Gromilov,[⊥] Inna K. Shundrina,[#] Renad Z. Sagdeev,[†] Matvey V. Fedin,^{*,†} and Elena G. Bagryanskaya^{*,†,#}

[†]International Tomography Center SB RAS, Institutskaya 3a, 630090 Novosibirsk, Russia

[‡]Novosibirsk State University, Pirogova 2, 630090 Novosibirsk, Russia

^{||}Borisevsk Institute of Catalysis SB RAS, Lavrentiev av. 5, 630090 Novosibirsk, Russia

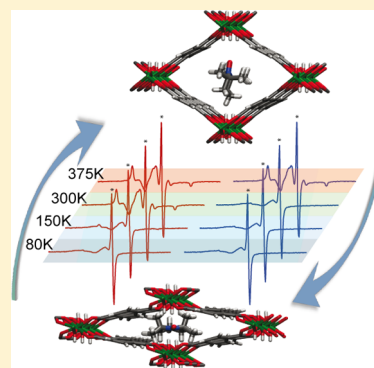
[⊥]Nikolaev Institute of Inorganic Chemistry SB RAS, Lavrentiev av. 3, 630090 Novosibirsk, Russia

[#]N.N. Vorozhtsov Novosibirsk Institute of Organic Chemistry SB RAS, Lavrentiev av. 9, 630090 Novosibirsk, Russia

S Supporting Information

ABSTRACT: Reversible structural rearrangements (“breathing”) of metal–organic frameworks (MOFs) are interesting and complex phenomena with many potential applications. They are often triggered by small amounts of adsorbed guest molecules; therefore, the guest–host interactions in breathing MOFs are intensively investigated. Due to the sensitivity limitations, most analytical methods require relatively high concentrations of guests in these studies. However, because guest molecules are not “innocent”, breathing behavior may become suppressed and unperturbed structural states inaccessible. We propose here the use of guest nitroxide molecules in tiny concentrations (such as 1 molecule per 1000 unit cells), which serve as spin probes for electron paramagnetic resonance (EPR), for effective study of breathing phenomena in MOFs. Using a perspective MIL-53(Al) framework as an example, we demonstrate the great advantage of this general approach, which avoids perturbation of the framework structure and allows in-depth investigation of guest–host interactions in the breathing mode.

SECTION: Spectroscopy, Photochemistry, and Excited States



Metal–organic frameworks (MOFs) made up of clusters or chains of metal ions connected by organic linkers have been intensively studied over the past decade.^{1,2} Three-dimensional (3D) porous frameworks, which may include 1D, 2D, and 3D channel systems, have intriguing structures, diverse topologies, and many potential applications, such as gas separation and storage, catalysis, ion exchange, microelectronics, health care, and so forth.^{3–5} Among others, a special interest has been drawn to flexible MOFs capable of reversible structural rearrangements under external stimuli, for example, temperature or guest–host interactions with adsorbed molecules.^{6,7} MIL-53(Al) built of the aluminum terephthalates is one of the impressive representatives of flexible MOFs, known to undergo temperature-induced structural transition with a significant hysteresis.^{8–12} The reversible changes (“breathing”) occur between large-pore (LP) and narrow-pore (NP) crystalline states with the cell volumes being 1427.5(3) and 863.9(2) Å³, respectively (Figure 1). In this work, we investigate structural dynamics and guest–host interactions in MIL-53(Al) using multifrequency (9/34 GHz) EPR of nitroxide spin probes. We demonstrate the great advantage of this approach, which combines the use of tiny concentrations of

probe molecules and high sensitivity of EPR and thus allows the investigation of unperturbed MOF structure and guest–host interactions in the breathing mode.

Previous studies of MIL-53(Al) and other flexible porous MOFs have shown that the adsorbed molecules may have a profound influence on their properties.^{13,14} In particular, a relatively small amount of adsorbed gases induces structural transitions and suppresses thermal “breathing” of MIL-53.^{10,15,16} We have prepared the samples of thin polycrystalline powder MIL-53(Al) containing probe radicals (2,2,6,6-tetramethylpiperidin-1-yl)oxyl (TEMPO) in ratios of 1/1000, 1/25, and 1/1 per unit cell of MIL-53(Al). The adsorption of nitroxide into a MOF was performed from the gas phase in anhydrous conditions, and the sample was then sealed in the quartz tube. However, only the “1/1000” sample retained its breathing properties, whereas at higher TEMPO concentrations, the breathing was suppressed, as evidenced by EPR (see below) and PXRD (Supporting Information). Therefore,

Received: November 1, 2013

Accepted: December 3, 2013

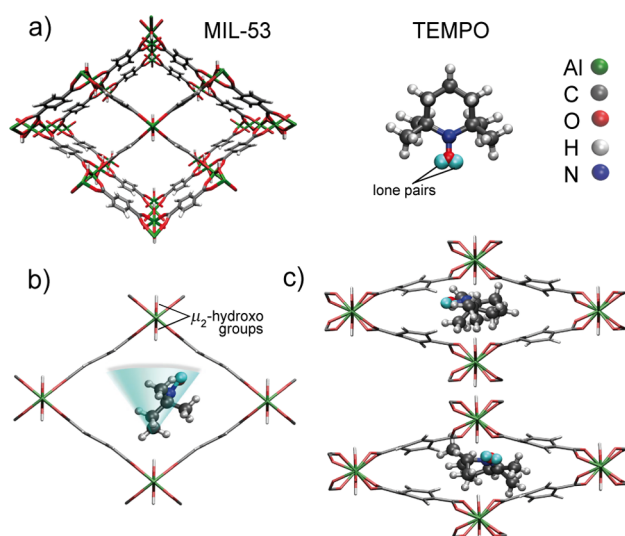


Figure 1. (a) Structures of MIL-53(Al) and TEMPO. (b) Illustration of TEMPO motion in large pores of MIL-53(Al) according to MD simulations. (c) Two representative locations of TEMPO in narrow pores of MIL-53(Al) with long (top) and short (bottom) distances from the NO group to the μ_2 -hydroxo group of MIL-53(Al) based on MD simulation results.

below, we focus on the 1/1000 sample and investigate its thermally induced behavior in detail.

Pure MIL-53(Al) exhibits structural transition between LP and NP states with a large thermal hysteresis; LP \rightarrow NP conversion occurs upon cooling at 125–150 K, whereas reverse NP \rightarrow LP conversion occurs upon warming between 325 and 375 K.^{11,12} In order to investigate correlations between these structural transitions and the molecular mobility of spin probes, we have measured EPR spectra at variable temperatures $T = 293$ –80 K both during cooling and warming of the sample (Figure 2). To ensure that the sample has reached thermal equilibrium during these experiments, at least 20 min of waiting time preceded each measurement. X-band continuous wave (CW) EPR spectra measured during cooling (Figure 2a) change dramatically from narrow-line pattern at room temperature to the typical spectrum of immobilized nitroxide at 80 K. Contrary to that, the spectra measured upon warming (Figure 2b) remain virtually unchanged with temperature and resemble those of immobilized nitroxide. Qualitatively, spectral changes during cooling can be explained by a consecutive conversion of MOF to the NP state, where the motion of nitroxide becomes strongly suppressed due to the volume restrictions. During heating, because of the large temperature hysteresis, MIL-53(Al) remains in the NP state up to 293 K; that is why EPR spectra retain the shape characteristic of immobilized nitroxides. If the sample is further warmed up to $T = 375$ K (NP \rightarrow LP transition of pure MIL-53(Al)) and then cooled down to 293 K, the spectrum returns to its initial shape. Thus, the structural transitions observed by means of the nitroxide probes are fully reversible and occur at similar temperatures as those previously observed for pure MIL-53(Al).^{11,12}

The changes of CW EPR spectra with temperature in the LP state can be reasonably well modeled assuming restricted molecular motion (MOMD model: microscopic order, macroscopic disorder),¹⁷ which approaches a nearly immobilized limit at 80 K (Figure 2; details in the Supporting Information). The principal values of tensors $\mathbf{g} = [2.0098 \ 2.0068 \ 2.0027]$ and $\mathbf{A} =$

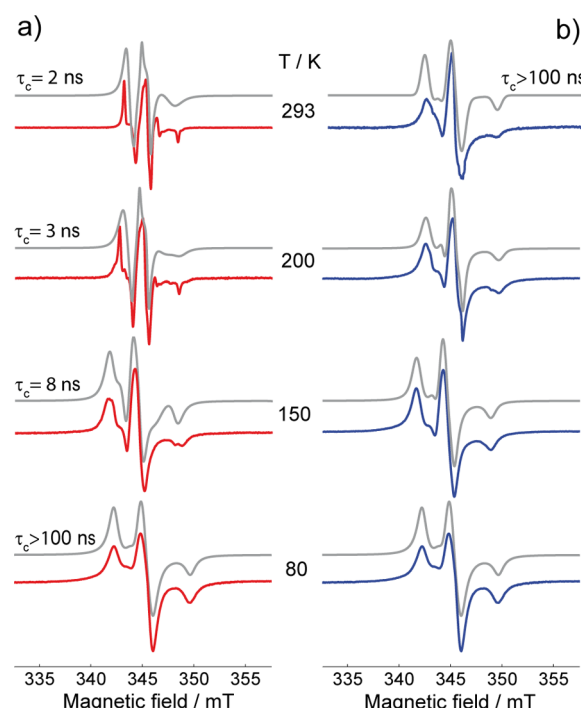


Figure 2. Variable-temperature X-band CW EPR spectra of TEMPO@MIL-53(Al) upon cooling down (a) and warming up (b). $\nu_{mw} \approx 9.7$ GHz. The intensity is given in au. Simulations are shown in gray, and obtained correlation times and values of temperature are indicated on the plot.

[0.65 0.65 3.70] mT (^{14}N hyperfine interaction) have been obtained from the data at 80 K and then used at all higher temperatures. The best agreement between calculated and experimental shapes was obtained using the parameters of orienting potential [$\lambda_{20} = 2$, $\lambda_{40} = 4$], justified by molecular dynamics (MD) simulations below (see also Figure S11 of the Supporting Information). Simultaneous fitting of X- and Q-band data (for the Q-band, see the Supporting Information) at each temperature allowed us to obtain the corresponding correlation times τ_c for nitroxide tumbling (Figure 2a). The agreement between theory and experiment at the sharp high-field features (Figure 2a, $T = 200$ –293 K) is not so good due to the imperfection of the orienting potential used (see the Supporting Information, Figure S11), but otherwise, the agreement is very reasonable. While at $T = 80$ K the nitroxide is immobilized, its τ_c value at room temperature approaches that typical of nitroxides freely rotating in viscous solutions.¹⁸ In the NP state, the situation is quite different, and EPR spectra at $T = 80$ –293 K (Figure 2b) can be well simulated assuming an immobile nitroxide, whose A_{zz} splitting slightly decreases with temperature (3.7 \rightarrow 3.5 mT at 80 \rightarrow 293 K). Such a decrease can be explained by intensive librations (small angle tumbling) of nitroxide growing in amplitude at higher temperature, which partially average anisotropic interactions.

Remarkably, the reversible changes of the spectrum shape (Figure 2) are accompanied by reversible changes of the second integral over the whole CW EPR spectrum (Figure 3), which is proportional to the number of spins in the sample. Each data point in Figure 3 has been collected using the following steps: (i) the sample has been placed in the cryostat or oil bath and stored (20 and 1 min, respectively) to reach the required temperature (indicated as the abscissa in Figure 3); (ii) the sample has been transferred to the probe head of the EPR

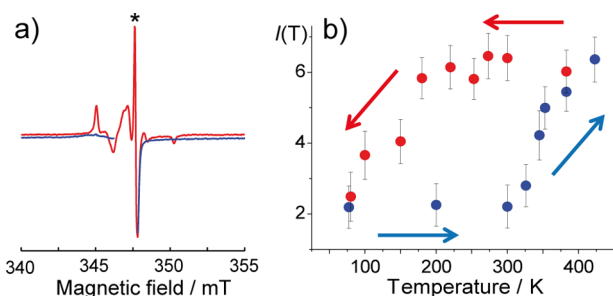


Figure 3. (a) Room-temperature EPR spectra of TEMPO@MIL-53(Al) in the LP (red —) and NP (blue —) states, normalized to the reference signal (*, DPPH). (b) The hysteresis loop measured using the second integral over the EPR spectrum $I(T)$ (values of I in au).

spectrometer; (iii) the EPR spectrum has been measured at room temperature together with the standard reference sample (DPPH, placed in a separate tube). Such an approach based on measurements in exactly the same experimental conditions and normalization to the reference provides reliable data for the second integral (see also the Supporting Information). The room temperature (293 K) lies within the hysteresis loop on its plateaus;^{11,12} therefore, the sample cannot “switch back” during its transfer from the experimental temperature to the detection (room) temperature. The obtained hysteresis loop for the second integral (Figure 3) agrees well with the structural hysteresis of pure MIL-53(Al).^{11,12} The value of the second integral decreases by a factor close to three upon transition to the NP state ($T = 80$ K) and reversibly switches back upon transition to the LP state ($T = 375$ K). The second integral over the EPR spectrum is proportional to the number of spins in the sample; thus, its pronounced changes during NP \leftrightarrow LP transitions indicate some reversible reaction involving nitroxide radicals.

Because the breathing mode can operate only for as small concentration of guest nitroxides as 1/1000 per u.c., many conventional techniques such as, for example, XRD/PXRD, NMR, and FTIR, cannot determine the structure of compounds/complexes formed by nitroxides. Therefore, the experimental structural investigation of the TEMPO@MIL-53(Al) system in the NP state is problematic. Still, on the basis of relevant literature data, theoretical calculations, and several indirect observations, plausible explanations can be proposed.

The reversible dimerization of nitroxides, which was previously observed in several studies,^{19,20} can be safely excluded for the 1/1000 sample due to the low concentration of nitroxides. Ananchenko et al. have investigated the supramolecular complex formation of TEMPO in nanocapsules of calix[4]arene.²¹ They found that TEMPO abstracts a hydrogen atom from a phenolic OH group of the amphiphilic *para*-hexanoylcalix[4]arene, and the hydroxylamine TEMPOH formed yields a stable inclusion complex with another molecule of the calixarene. Single crystals with 100% of the nanocapsules being occupied by TEMPOH had been obtained that allowed definite conclusions on the structure based on X-ray data. Although in that case the complex formation was irreversible, the situation is in many respects similar to the presently studied TEMPO@MIL-53(Al). In addition, there are examples of hydrogen atom abstraction by TEMPO from metal complexes, including the observation of an unusual increase of the reaction rate at low temperature.²² Therefore, we assume that a formation of TEMPOH in narrow pores of MIL-53(Al) is a

reason for the disappearance of $\sim 2/3$ of nitroxide spins upon transition to the NP state.

To determine energetically preferential TEMPO locations in NP and LP states, we have performed MD simulations. The local perturbation of the MIL-53(Al) structure by adsorbed nitroxide has been neglected for simplicity, and the electrostatic and van der Waals (vdW) terms for MIL-53(Al) were taken from the literature.²³ An ab initio parametrization force field for TEMPO was kindly provided by the authors of ref 24. As usual, for molecular mechanics, in this parametrization, two lone pairs (lp's) of TEMPO have been positioned at 0.45 Å from the oxygen atom, with NO...lp angle being 120°. We describe the observed restricted motion of TEMPO in LP and NP states and provide illustrative gif movies (see the Supporting Information), whereas Figure 1 shows representative orientations. An intensive tumbling of TEMPO is found in the LP state; however, a certain range of orientations with the NO group approaching the OH group of MIL-53(Al) is not accessible. The shortest (N)O...H(O) distances are ~ 2.2 – 2.5 Å, which is too large for TEMPOH formation. On the other hand, in the NP state, TEMPO is tightly squeezed by the MOF, and only local librations are allowed within a narrow range of orientations. Both conclusions are in full agreement with the CW EPR data/simulations shown above (Figure 2; Supporting Information). The calculations for the NP state, however, are simplified because the size of the narrow pore is comparable with the size of nitroxide, and thus, local perturbation of the MOF and nitroxide structures is quite possible. Calculations show that nitroxide can be trapped in a number of orientations, where the piperidine ring of TEMPO lies closely parallel to the plane containing the long axis of the lozenge and direction of the nanochannel (horizontal plane in Figure 1c). For example, when the NO group is oriented across the nanochannel, the (N)O...H(O) distance is ~ 3 Å (Figure 1c, top); at the same time, when the NO group is directed along the nanochannel, the (N)O...H(O) distance is ~ 1.1 Å (Figure 1c, bottom), which makes the complex formation between TEMPO and MIL-53(Al) via μ_2 -hydroxo groups quite possible. Thus, for a certain range of orientations of nitroxide trapped in narrow pores, the bonding with MIL-53(Al) is possible, whereas for the others, it is not. Obtaining the exact proportion between these two fractions is currently not feasible because calculation of the LP \rightarrow NP transition of the whole flexible MOF/nitroxide system is a very difficult task. Still, the above MD calculations clearly showed that (i) nitroxide intensively tumbles in the LP state, and the orientations favorable for (N)O...H(O) bond formation are sterically hindered and (ii) nitroxide can be trapped in different orientations in the NP state, some of which allow for (N)O...H(O) bonding.

The formation of hydroxylamine TEMPOH may, in principle, occur via hydrogen atom transfer (HAT) or proton-coupled electron transfer (PCET) mechanisms,^{26,27} and mutual orientations of TEMPO and the μ_2 -hydroxo group of MIL-53(Al) in the NP state presume the PCET mechanism. When diamagnetic TEMPOH is formed, the electron spin density should pass to the $\text{AlO}_4(\text{OH})\text{O}^\bullet$ type radical, which was not detected by EPR even at $T < 10$ K, perhaps due to a very short relaxation time known for Al-centered radicals.²⁸ Note that reverse reaction of TEMPO formation upon transition from the NP to LP state occurs only after the heating to 375 K (NP \rightarrow LP transition temperature). We suppose that the two factors, the change of the MIL-53(Al) structure and the increase of the temperature, make TEMPOH

unstable, and thus, the hydrogen atom returns back to the μ_2 -hydroxo group.

In addition to the above theoretical reasoning, several experimental observations confirm, though indirectly, the interaction between TEMPO and the μ_2 -hydroxo group of MIL-53(Al). First, we have also performed variable-temperature pulse EPR measurements. It is worth noting that intense electron spin echo signals have been observed in both LP and NP states even at room temperature. The first derivatives of echo-detected EPR spectra are very close to CW EPR spectra (Supporting Information). In order to probe the local environment of the nitroxide inside of MIL-53(Al), we obtained HSCORE spectra in LP and NP states (at 200 and 80 K, respectively). The spectra are very similar in both states and show only diagonal peaks corresponding to hyperfine interaction of the electron with remote protons (14.8 MHz) and Al nuclei (3.8 MHz) (Supporting Information). Note that only those TEMPO radicals that have not converted to TEMPOH in the NP state ($\sim 1/3$) can be observed by EPR. Interaction of adsorbed nitroxide with aluminum nuclei clearly indicates that the NO group of TEMPO is located close to the $\text{AlO}_4(\text{OH})_2$ octahedron inside of the channels. In addition, complementary FTIR, PXRD, and TGA measurements (which can only be implemented for highly concentrated samples with suppressed breathing) all indicate interaction of TEMPO with MIL-53(Al) via a (N)O \cdots H(O) link (Supporting Information).

In conclusion, we have demonstrated that EPR of nitroxide spin probes is a choice method for studying structural dynamics and guest–host interactions in switchable flexible MOFs. The information is readily obtained from analyses of spin probe mobility and complexation with MOFs. The low probe concentrations combined with high sensitivity of EPR allow the investigation of the guest–host system in the breathing mode, which is not feasible for most of the other analytical methods such as NMR, PXRD, DSC/TGA, and so forth at similar guest concentrations. Therefore, the potential of the approach presented here is unquestionable for the future studies of promising MOFs and their applications, and some of these studies are already underway.

EXPERIMENTAL SECTION

The hydrothermal synthesis of MIL-53 was described previously.^{29–31} MIL-53(Al) powder (30 mg) was placed in a closed vacuum system and evacuated at 10^{-5} Torr for 2 h at room temperature; afterward, it was maintained for 12 h at 150 °C to eliminate the remaining water from the MOF. The adsorption of nitroxide into the MOF was performed at room temperature from the gas phase (the equilibrium vapor pressure at room temperature is ~ 0.8 Torr for TEMPO), and the sample was then sealed in the quartz tube. CW and pulse X/Q-Band EPR spectra were measured using Bruker EMX and Bruker Elexsys E580 spectrometers, the latter equipped with an Oxford temperature control system. Simulations of EPR spectra were performed using the Easyspin toolbox (version 4.5.1) for Matlab³² and MD simulations using the Gromacs-MD package.³³ For more experimental details, see the Supporting Information.

ASSOCIATED CONTENT

Supporting Information

Experimental procedures, supplementary EPR data (Figures S1–S3), HSCORE spectra (Figure S4), PXRD spectra (Figures S5 and S6), FTIR spectra (Figures S7 and S8),

TGA data (Figure S9), and details of MD simulations (Figures S10 and S11) are included. This material is available free of charge via the Internet at <http://pubs.acs.org>.

AUTHOR INFORMATION

Corresponding Authors

*E-mail: mfedin@tomo.nsc.ru (M.V.F.).

*E-mail: egbagryanskaya@nioch.nsc.ru (E.G.B.).

Notes

The authors declare no competing financial interest.

ACKNOWLEDGMENTS

This work was supported by RFBR (12-03-33010, 12-03-31329), Div. Chem. Mater. Sci. RAS (No. 5.1.1), and The Ministry of Education and Science of Russian Federation (Projects 8436 and 8456). We thank Prof. Sylvain Marqu  for fruitful discussions.

REFERENCES

- (1) F  rey, G. Hybrid Porous Solids: Past, Present, Future. *Chem. Soc. Rev.* **2008**, *37*, 191–214.
- (2) Zhou, H. C.; Long, J. R.; Yaghi, O. M. Introduction to Metal–Organic Frameworks. *Chem. Rev.* **2012**, *112*, 673–674.
- (3) Tanabe, K. K.; Cohen, S. M. Engineering a Metal–Organic Framework Catalyst by Using Postsynthetic Modification. *Angew. Chem., Int. Ed.* **2009**, *48*, 7424–7427.
- (4) Nijem, N.; Wu, H. H.; Canepa, P.; Marti, A.; Balkus, K. J.; Thonhauser, T.; Li, J.; Chabal, Y. J. Tuning the Gate Opening Pressure of Metal–Organic Frameworks (MOFs) for the Selective Separation of Hydrocarbons. *J. Am. Chem. Soc.* **2012**, *134*, 15201–15204.
- (5) Sun, F.; Yin, Z.; Wang, Q. Q.; Sun, D.; Zeng, M. H.; Kurmoo, M. Tandem Postsynthetic Modification of a Metal–Organic Framework by Thermal Elimination and Subsequent Bromination: Effects on Absorption Properties and Photoluminescence. *Angew. Chem., Int. Ed.* **2013**, *52*, 4538–4543.
- (6) Fernandez, C. A.; Thallapally, P. K.; Motkuri, R. K.; Nune, S. K.; Sumrak, J. C.; Tian, J.; Liu, J. Gas-Induced Expansion and Contraction of a Fluorinated Metal–Organic Framework. *Cryst. Growth Des.* **2010**, *10*, 1037–1039.
- (7) Chen, L.; Mowat, J. P. S.; Fairen-Jimenez, D.; Morrison, C. A.; Thompson, S. P.; Wright, P. A.; D  ren, T. Elucidating the Breathing of the Metal–Organic Framework MIL-53(Sc) with Ab Initio Molecular Dynamics Simulations and In Situ X-ray Powder Diffraction Experiments. *J. Am. Chem. Soc.* **2013**, *135*, 15763–15773.
- (8) F  rey, G.; Latroche, M.; Serre, C.; Millange, F.; Loiseau, T.; Percheron-Guegan, A. Hydrogen Adsorption in the Nanoporous Metal–Benzenedicarboxylate $\text{M}(\text{OH})(\text{O}_2\text{C}-\text{C}_6\text{H}_4-\text{CO}_2)$ ($\text{M} = \text{Al}^{3+}$, Cr^{3+}), MIL-53. *Chem. Commun.* **2003**, 2976–2977.
- (9) F  rey, G.; Serre, C. Large Breathing Effects in Three-Dimensional Porous Hybrid Matter: Facts, Analyses, Rules and Consequences. *Chem. Soc. Rev.* **2009**, *38*, 1380–1399.
- (10) Coudert, F. X.; Mellot-Draznieks, C.; Fuchs, A. H.; Boutin, A. Double Structural Transition in Hybrid Material MIL-53 upon Hydrocarbon Adsorption: The Thermodynamics Behind the Scenes. *J. Am. Chem. Soc.* **2009**, *131*, 3442.
- (11) Liu, Y.; Her, J. H.; Dailly, A.; Ramirez-Cuesta, A. J.; Neumann, D. A.; Brown, C. M. Reversible Structural Transition in MIL-53 with Large Temperature Hysteresis. *J. Am. Chem. Soc.* **2008**, *130*, 11813–11818.
- (12) Mendt, M.; Jee, B.; Stock, N.; Ahnfeldt, T.; Hartmann, M.; Himsl, D.; Poppl, A. Structural Phase Transitions and Thermal Hysteresis in the Metal–Organic Framework Compound MIL-53 As Studied by Electron Spin Resonance Spectroscopy. *J. Phys. Chem. C* **2010**, *114*, 19443–19451.
- (13) Potts, S. V.; Barbour, L. J.; Haynes, D. A.; Rawson, J. M.; Lloyd, G. O. Inclusion of Thiazyl Radicals in Porous Crystalline Materials. *J. Am. Chem. Soc.* **2011**, *133*, 12948–12951.

- (14) Rallapalli, P.; Prasanth, K. P.; Patil, D.; Somani, R. S.; Jasra, R. V.; Bajaj, H. C. Sorption Studies of CO₂, CH₄, N₂, CO, O₂ and Ar on Nanoporous Aluminum Terephthalate MIL-53(Al). *J. Porous Mater.* **2011**, *18*, 205–210.
- (15) Llewellyn, P. L.; Maurin, G.; Devic, T.; Loera-Serna, S.; Rosenbach, N.; Serre, C.; Bourrelly, S.; Horcajada, P.; Filinchuk, Y.; Férey, G. Prediction of the Conditions for Breathing of Metal Organic Framework Materials Using a Combination of X-ray Powder Diffraction, Microcalorimetry, And Molecular Simulation. *J. Am. Chem. Soc.* **2008**, *130*, 12808–12814.
- (16) Bourrelly, S.; Moulin, B.; Rivera, A.; Maurin, G.; Devautour-Vino, S.; Serre, C.; Devic, T.; Horcajada, P.; Vimont, A.; Clet, G.; et al. Explanation of the Adsorption of Polar Vapors in the Highly Flexible Metal Organic Framework MIL-53(Cr). *J. Am. Chem. Soc.* **2010**, *132*, 9488–9498.
- (17) Moro, G.; Freed, J. H. Efficient Computation of Magnetic-Resonance Spectra and Related Correlation-Functions from Stochastic Liouville Equations. *J. Phys. Chem.* **1980**, *84*, 2837–2840.
- (18) Herrmann, W.; Stosser, R.; Moll, K. P.; Borchert, H. H. Rates of Rotational Diffusion and Heisenberg Spin Exchange As Obtained from CW ESR and ESR Tomographic Experiments on Model Systems and Human Skin. *Appl. Magn. Reson.* **2005**, *28*, 85–106.
- (19) Bowman, D. F.; Gillan, T.; Ingold, K. U. Kinetic Applications of Electron Paramagnetic Resonance Spectroscopy. III. Self-Reactions of Dialkyl Nitroxide Radicals. *J. Am. Chem. Soc.* **1971**, *93*, 6555–6561.
- (20) Mendenhall, G. D.; Ingold, K. U. Reversible Dimerization and Some Solid-State Properties of Two Bicyclic Nitroxides. *J. Am. Chem. Soc.* **1973**, *95*, 6390–6394.
- (21) Ananchenko, G. S.; Pojarova, M.; Udachin, K. A.; Leek, D. M.; Coleman, A. W.; Ripmeester, J. A. Supramolecular Stabilization of Hydroxylamine TEMPOH by Complexation with an Amphiphilic Calixarene. *Chem. Commun.* **2006**, 386–388.
- (22) Mayer, J. M. Understanding Hydrogen Atom Transfer: From Bond Strengths to Marcus Theory. *Acc. Chem. Res.* **2011**, *44*, 36–46.
- (23) Vanduyfhuys, L.; Verstraelen, T.; Vandichel, M.; Waroquier, M.; Van Speybroeck, V. Ab Initio Parametrized Force Field for the Flexible Metal–Organic Framework MIL-53(Al). *J. Chem. Theory Comput.* **2012**, *8*, 3217–3231.
- (24) Stendardo, E.; Pedone, A.; Cimino, P.; Menziani, M. C.; Crescenzi, O.; Barone, V. Extension of the AMBER Force-Field for the Study of Large Nitroxides in Condensed Phases: An Ab Initio Parameterization. *Phys. Chem. Chem. Phys.* **2010**, *12*, 11697–11709.
- (25) Dixon, R. W.; Kollman, P. A. Advancing beyond the Atom-Centered Model in Additive and Nonadditive Molecular Mechanics. *J. Comput. Chem.* **1997**, *18*, 1632–1646.
- (26) Warren, J. J.; Tronic, T. A.; Mayer, J. M. Thermochemistry of Proton-Coupled Electron Transfer Reagents and Its Implications. *Chem. Rev.* **2010**, *110*, 6961–7001.
- (27) Mader, E. A.; Davidson, E. R.; Mayer, J. M. Large Ground-State Entropy Changes for Hydrogen Atom Transfer Reactions of Iron Complexes. *J. Am. Chem. Soc.* **2007**, *129*, 5153–5166.
- (28) Claridge, R. F. C.; Mackle, K. M.; Sutton, G. L. A.; Tennant, W. C. 10-K EPR of an Oxygen–Hole Aluminum Center, AlO₄(0), in X-Irradiated Zircon, ZrSiO₄. *J. Phys.: Condens. Matter* **1994**, *6*, 10415–10422.
- (29) Loiseau, T.; Serre, C.; Huguenard, C.; Fink, G.; Taulelle, F.; Henry, M.; Bataille, T.; Férey, G. A Rationale for the Large Breathing of the Porous Aluminum Terephthalate (MIL-53) upon Hydration. *Chem.—Eur. J.* **2004**, *10*, 1373–1382.
- (30) Lieder, C.; Opelt, S.; Dyballa, M.; Henning, H.; Klemm, E.; Hunger, M. Adsorbate Effect on AlO₄(OH)₂ Centers in the Metal–Organic Framework MIL-53 Investigated by Solid-State NMR Spectroscopy. *J. Phys. Chem. C* **2010**, *114*, 16596–16602.
- (31) Alaerts, L.; Maes, M.; Giebel, L.; Jacobs, P. A.; Martens, J. A.; Denayer, J. F. M.; Kirschhock, C. E. A.; De Vos, D. E. Selective Adsorption and Separation of ortho-Substituted Alkylaromatics with the Microporous Aluminum Terephthalate MIL-53. *J. Am. Chem. Soc.* **2008**, *130*, 14170–14178.
- (32) Stoll, S.; Schweiger, A. EasySpin, a Comprehensive Software Package for Spectral Simulation and Analysis in EPR. *J. Magn. Reson.* **2006**, *178*, 42–55.
- (33) Pronk, S.; Pall, S.; Schulz, R.; Larsson, P.; Bjelkmar, P.; Apostolov, R.; Shirts, M. R.; Smith, J. C.; Kasson, P. M.; van der Spoel, D.; et al. GROMACS 4.5: A High-Throughput and Highly Parallel Open Source Molecular Simulation Toolkit. *Bioinformatics* **2013**, *29*, 845–854.